CERTIFICATION OF APPROVAL

Effect Of Nanoparticle Crystallite Sizes In A Nanofluid On The Interfacial Tension Of Oil For Oil Recovery In EOR

by

Mohd Adnan Bin Saidin

A project dissertation submitted to the
Petroleum Engineering Programme
Universiti Teknologi PETRONAS
in partial fulfilment of the requirements for the
BACHELOR OF ENGINEERING (Hons)
(PETROLEUM ENGINEERING)

Approved by,

_____
(Dr. Hasnah Mohd Zaid)

UNIVERSITI TEKNOLOGI PETRONAS
TRONOH, PERAK
2013

CERTIFICATION OF ORIGINALITY

This is to certify that I am responsible for the work submitted in this project, that the original work is my own except as specified in the references and acknowledgements, and that the original work contained herein have not been undertaken or done by unspecified sources or persons.

_____

MOHD ADNAN BIN SAIDIN

ABSTRACT

Oil production are decreasing from days to days. Hence, Enhanced Oil Recovery (EOR) have been developed to maximize the production. EOR is not a new thing in oil and gas industry. EOR which consist of several collection of technologies-involving the use of thermal, gas and chemicals means for producing more oil. Nanotechnology is one of the advanced technology that finding its place in EOR process as it provides a high potential for oil and gas recovery. This can be shown from recent research projects that nanotechnology has the potential to solve several problems in the petroleum industry. Recent studies shows that, Aluminum oxide nanoparticles for example, has been proved as it can improved the oil recovery. However, the sizes of the nanoparticles will also contribute to the effect on the interfacial tension of oil. Therefore, to find out the effect of this nanoparticle sizes is the primary objective in this study. In this study, aluminum oxide (Al_2O_3) nanoparticles is used and the experimental study on the effect of this nanoparticle sizes in a nanofluid on the interfacial tension of oil is conducted under surface conditions. Four samples of different average crystallite size were used to study the effect of particle size on the oil recovery. The results obtained from this experiment indicate that the Al_2O_3 nanoparticles are good agents for EOR and Al_2O_3 nanofluid which consists of average crystallite size of 14-18nm reduces the interfacial tension (IFT) between crude oil and water and gives the highest recovery of 43% ROIP.

ACKNOWLEDGEMENTS

Alhamdulillah, all praises to Allah Subhanahu Wa Ta'ala for the blessing and strength that He has given to me to search for knowledge throughout completing this project.

First and foremost, I would like to take this opportunity to express my gratitude and appreciation to my project supervisor, Dr. Hasnah Mohd Zaid who had continuously monitored the progress throughout FYPI and FYPII timeline. Her constructive comments and advices, continuous positive support and guidance and good suggestions towards project enhancement have guided the project towards a successful final outcome.

I also wish to thank Noor Rasyada Ahmad Latiff as my co-supervisor for her assistance, continuous assistance, support and invaluable guidance throughout the project. Thanks Kak for being awesome!

This appreciation is also dedicated to Universiti Teknologi PETRONAS (UTP) especially to the committee of Final Year Project of Petroleum Engineering department for excellent organization and management of this course. Besides, I would also like to acknowledge the staffs and technician of Central Analytical Lab, Mechanical Engineering Department, Fundamental & Applied Sciences Department, Petroleum Engineering Department and Chemical Engineering Department of Universiti Teknologi PETRONAS for their kindness and supportive encouragement throughout completion of this project.

Last but not least, I would also like to thank all people who have helped and inspired me during my research study. My deepest gratitude also goes to my family for their support throughout my life. Million thanks to all my fellow friends who always been very supportive and helpful throughout the journey.

Many thanks to all others not mentioned here individually.

TABLE OF CONTENTS

LIST OF FIGURES

LIST OF FIGURES

CHAPTER 1

INTRODUCTION

1.1 Background Of Study

According to U.S. Energy Information Administration (EIA), they project that world energy consumption will increase 56% by 2040[2]. Fossil fuels energy still remains an ultimate source of energy as shown in **Figure 1.**

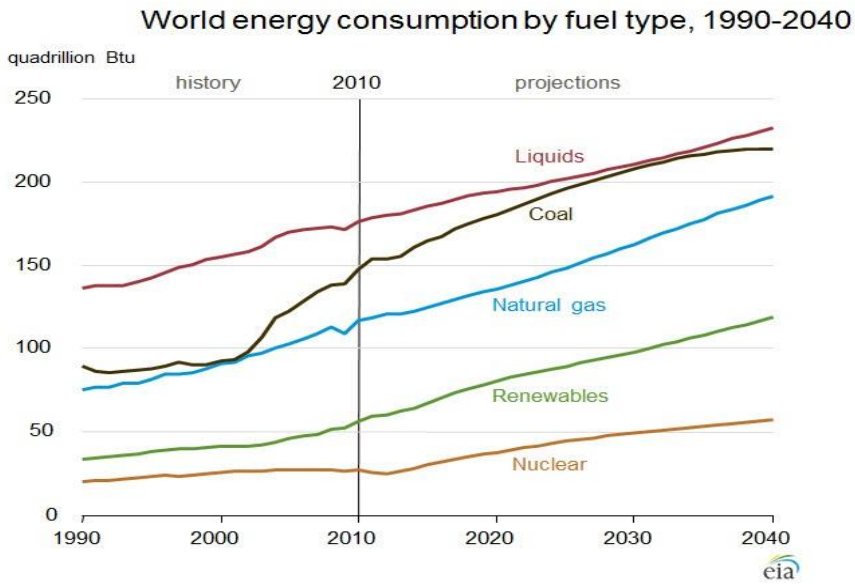

Figure 1: World energy consumption by fuel type 1990-2040[3]

Figure 1 shows that the demand in fossil fuels as energy demand keeps increasing from time to time. As for now, 85% of all energy produced in the United States comes from burning these fuels and the energy is used to power up almost two thirds of electricity and transportation[3]. However, in 2008, World Economic Outlook (WEO) states that the oil production from the existing fields are decreasing and shows a declining trend in the discovery of the new conventional oil reserves as shown in **Figure 2**[4]**.**

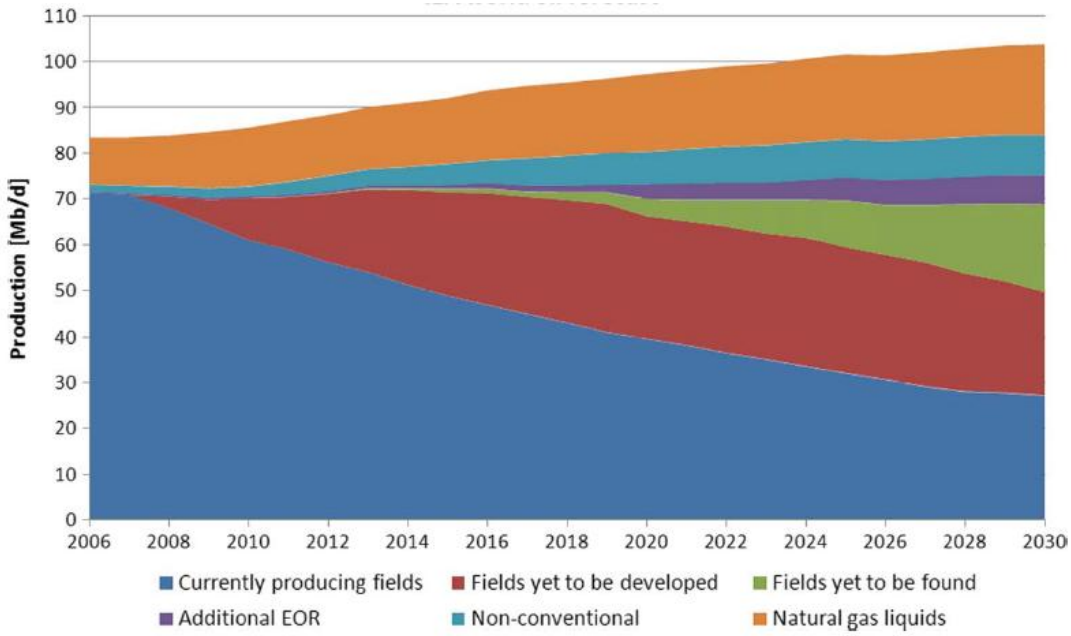

Figure 2: World Oil production from World Energy Outlook 2008 [4]

Conventional and unconventional oil are the terms that are used to describe the type of the oil reservoir. Conventional oil is the oil that can be easily recovered with low cost and without using any advanced technology. This oil can be easily produced by using primary and secondary recovery method. While the unconventional oil is the oil that is not cost effective to produce by conventional method such as heavy oil, deepwater reservoir, unconsolidated formation and high temperature and high pressure (HTHP) reservoir. Nowadays, the conventional oil reservoir is depleted and most of the new discovered reservoirs are categorized as unconventional oil reservoir [5]. Due to the high in oil demand, this unconventional oil is need to be recovered and a new highly advanced technology such as tertiary recovery method or Enhanced Oil Recovery (EOR) has to be implemented.

In order to produce oil from the reservoir, there are three stages of recovery need to be carried out which are primary, secondary, and tertiary recovery as shown in **Figure 3**. Primary recovery is the first oil that comes out from the reservoir after drilling activity took place. This recovery uses the natural pressure of the reservoir to push the crude oil to the surface. By using this recovery method, usually 10 - 15% of oil is being recovered from the original oil in place (OOIP)[6].

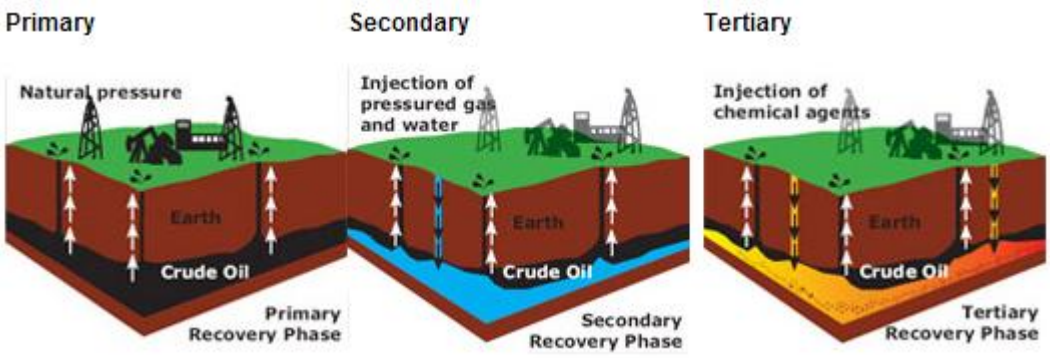

Figure 3: Oil Recovery Stages[29]

Secondary recovery will be applied after the natural pressure of the reservoir has decreases and unable to push the remaining oil. In secondary recovery phase, pressurized gas and water will be injected into the reservoir to drive residual crude oil and remaining gas to the surface wells. The most common methods being used in secondary recovery phase are gas injection and water flooding. The gas is injected into the gas cap while the water is injected into the production zone to sweep oil from the reservoir [7]. The secondary stage will reach its limit when the injected water or gas is being produced in a considerable amount which is no longer economical. Secondary recovery allows additional 10-20% of OOIP. S.Thomas (2007) found that, Primary and secondary recovery only constitute 33% of oil initially in place, leaving 67% behind [8].

Finally, tertiary oil recovery phase will be carried out. In tertiary recovery phase or also known as Enhanced Oil Recovery (EOR), different chemical agents and materials will be injected to improve the flow between the oil, gas and rock and to recover remaining crude oil after primary and secondary recovery phase. Tertiary recovery allows additional 20% to 30% of oil to be recovered from the reservoir. There are 4 well known EOR techniques which are chemical, thermal, microbial and gas injection.

However there are some limitation in EOR methods application. In order to recover oil from HTHP reservoirs, consideration has to be taken on methods which

have applicability to operate at these extreme conditions. One criteria that should be considered are the sustainability of the agent in the extreme pressure and temperature environment. In this case, the agent is the injectant or external fluid to be injected into the reservoir to stimulate oil recovery.

When dealing with HTHP environment, some of the EOR methods are not feasible as for example, chemical flooding method. This is because the chemicals used for example surfactant and polymer that is used to reduce interfacial tension between oil and water interface and also to increase the sweep efficiency of the displacing fluid, are not able to withstand high temperature. However, in this study, this problem will be treated by injecting nanoparticles suspension into the porous medium.

The application of nanotechnology in oil and gas industry has given a big impact on oil recovery as recent research projects had shown that nanotechnology has potential to increase oil and gas production. This is because nanoparticles have the ability to alter certain factors in the formation and can withstand the HTHP environment that can be used to enhance recovery. The uses of nanoparticles in oil and gas production has been reported by several authors and will be discussed in the next chapter.

The main objective of this work is to study the effect of nanoparticle sizes in nanofluid on the interfacial tension of oil on EOR since the sizes may affect the oil recovery. In order to analyze the nanoparticle sizes, an experiment will be conducted in two phases. First is to synthesize the nanoparticles and characterize the properties such as particle size, crystallite size and the morphology. Second phase is to analyze the size of the nanoparticle that can affect the most on interfacial tension of oil and can give the optimum oil recovery. The results of this project will be a reference for future researches in nanotechnology of oil and gas industries.

1.2 Problem Statement

As discussed earlier, some criterion should be taken into consideration in order to design new EOR method that is suitable for unconventional oil. Other EOR methods have some limitation due to cost effectiveness and not suitable for HTHP formation condition that can cause failure to electronic devices as well as alter the stability of the injecting stimulating agents or fluids into the reservoir. Therefore the injection of nanoparticles which are dispersed in nanofluid, which is to reduce interfacial tension between oil and water interface and also to increase the sweep efficiency of the displacing fluid in the formation will be used for the EOR method.

All the recent studies have failed to provide the ideal nanoparticle crystallite size that will contribute to the most oil recovery. Hence, in this study, the ideal crystallite size that stimulate the oil production and give the most oil recovery will be determined.

1.3 Objectives

The purpose of this work is :-

i. to synthesize Aluminium Oxide Al_2O_3 nanoparticles and characterize its properties.

ii. to determine how the Al_2O_3 nanoparticle crystallite sizes affect the interfacial tension of oil

iii. to determine how the Al_2O_3 nanoparticle crystallite sizes affect the oil recovery in EOR

1.4 Scope of works

In this study, the scope of works will include the synthesis and characterizations of the Al_2O_3 nanoparticles. This Al_2O_3 will be synthesized by using sol-gel method and the micro structural of the Al_2O_3 will be analyzed using x-ray diffraction (XRD), field emission scanning electron microscopy (FESEM), energy dispersed x-ray (EDX) and transmission electron microscopy (TEM).

The nanoparticles of different sizes are then dispersed in base fluid to form nanofluids and will act as the surfactant or injecting fluid during core flooding procedure. The porous medium prepared will be characterized for its properties e.g. porosity permeability and pore volume. Properties of the crude oil used in this experiment will also be characterized.

Experiments will be conducted at surface condition which is at room temperature and at atmospheric pressure. Silica beads will be used as the porous medium and the coreflooding experiment setup will be discussed further in the next chapter. The interfacial tension (IFT) between the oil and nanofluids are also will be measured by using the Spinning Drop Tensionmeter.

CHAPTER 2
LITERATURE REVIEW

2.1 Literature Review

Basically, EOR is any method that can be used to extract liquid hydrocarbon from the reservoir after its production from primary and secondary production has been significantly halt or depleted. S.Thomas (2007) found that, primary and secondary recovery only constitute 33% of oil initially in place, leaving 67% behind. It is estimated that approximately 2.0×10^{12} barrels of conventional oil and 5.0×10^{12} barrels of heavy oil remains in reservoir worldwide after conventional recovery method have been exhausted [8]. This oil can be recovered by EOR methods, however, the choice of the method is highly depend on many consideration because of oil reservoir is associated with a large number of variables such as crude oil type, viscosity, pressure and temperature.

Lake et al, (1992) claimed that there are three main categories of EOR which are thermal, chemical and miscible or immiscible gas [9]. Steam flooding, in-situ combustion, and EM heating are some of the EOR thermal method. Thermal energy is used to heat up the oil formation and therefore reducing the oil viscosity. Chemical EOR includes the use of polymers, surfactants and alkali. This method work either by reducing the IFT between oil and water, increasing sweep efficiency or changing the reservoir rock wettability. There are some limitation when dealing with chemical EOR which is, for example, polymers are not able to withstand high temperature as well as high in cost and quantity required.

Nanoparticles has been gaining much attention due to its potential to solve or manage several problems in the petroleum industry. Recent studies on wettability formation shows that wettability water wet formations produce better than oil wet formation and the wettability of a formation can be altered by nanoparticles.

Dong et al, (2006) concluded that intermediately wet formation produce better than water wet formation[1]. Wettability of a reservoir rock can be defined as the ability of one fluid in the presence of another to spread onto the surface of the rocks. Wettability is very important in the production of oil and gas because it is the main factor in the flow processes in the formation as well as to determine the initial fluid distribution [10].

The use of nanoparticles and its effect on oil recovery has been reported by several authors for example silicon oxide (nanoparticles) dispersed in ethanol to form nanofluid come out with a good oil recovery results on water wet formation [11]. The study by Onyekonwu et al concluded that there are three different types of polysilicon nanoparticles (PSNP) that can change the wettability of a rock surface differently. Lipophobic and hydrophilic PSNP (LHPN) can turn an oil wet rock or make an already water wet rock strongly water wet. Hydrophobic and lipophilic PSNP (HLPN) can render water wet rock oil wet or make an already oil wet rock strongly oil wet. And lastly, neutrally wet PSNP (NWPN) can change either oil or water wet formation to an intermediate state [11].

Nanoparticles also can decrease the oil viscosity. There are several types of nanoparticles which are aluminum oxides, zinc oxides, magnesium oxides, iron oxides, silicon oxides and others. N.A. Ogolo et al, (2012) underline that aluminum oxide is the good agent for EOR in reducing the IFT between the oil and water[12]. Interfacial tension is defined as the boundary tension between two immiscible liquids. There are several properties that influence the interfacial tension between two liquid phases which are viscosity, thermal conductivity, density, boiling and freezing points. Interfacial tension can greatly influence the other important rock properties such as wettability, relative permeability and capillary pressure [13]. Reduction in oil-water interfacial tension can help to increase oil production using EOR method. One of the method being used to lower the interfacial tension is through chemical injection into the oil reservoir. In a study done by Dong et al, it was proven that there is a reaction between alkali and acidic components in the crude oil which reduces the interfacial

tension between the oil and water by injecting alkaline solution which is sodium hydroxide into the porous medium[14].

More recent evidence in the positive effect of nanoparticles on oil recovery come from Wasan and Nikolov (2003). They shows that, nanoparticles in nanofluid tend to assemble themselves into structural arrays at a discontinuous phase such as oil, gas, paraffin, or polymer. The particles tend to form a wedge-like structure and force themselves between the discontinuous phase on the solid surface [15]. The wedge effect is shown in **Figure 4.**

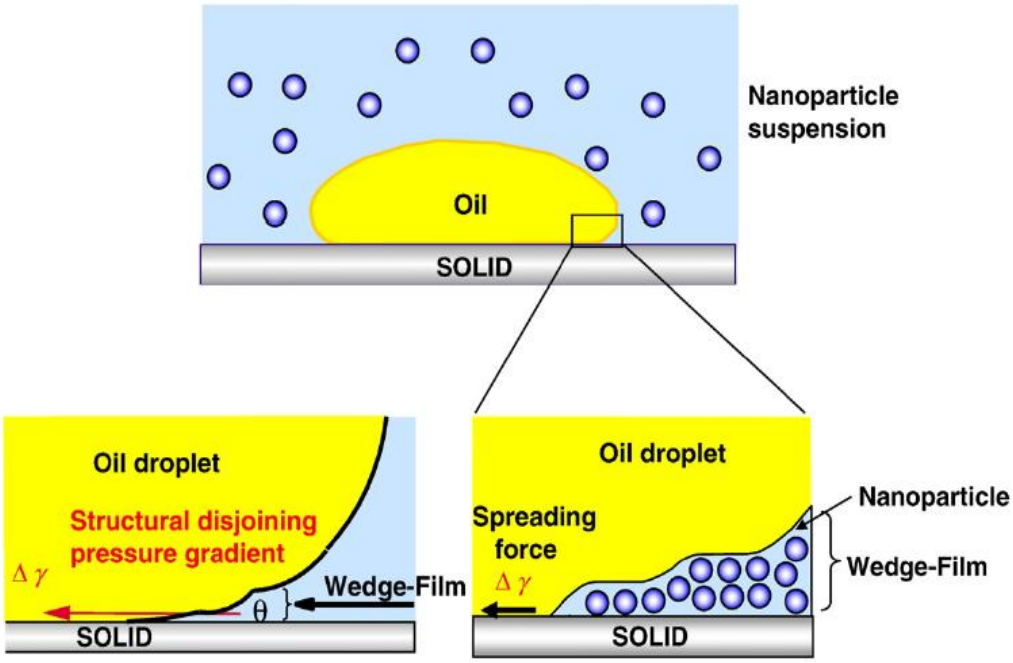

Figure 4: This illustrates the wedge effect resulting in structural disjoining pressure[15].

The force is called the disjoining pressure force and the force from a single particle is very weak but as large amount of small particles are present, the force will be increased. As the force increases, the oil will be displaced. From this disjoining pressure theory, nanoparticles enables nanofluid to act as wetting agents and as interfacial surface reducers [15].

Nanofluid can influence the interfacial tension between crude oil and fluid in the reservoir. Nanofluid is able to increase oil recovery by reducing the interfacial tension between oil and brine/nanofluids. The higher concentration of

nanofluid also could contribute to higher disjoining pressure which causes more oil to be produced from the reservoir. When the interfacial tension decreases, the curve of oil-water relative permeability system will be more straight lines. So therefore, it will be easier for the oil to move out since the friction force between water-phase and oil-phase also reduced[16].

All the previous researches were conducted to see the effect of nanoparticles in a nanofluid on the viscosity and interfacial tension of oil for EOR, however the ideal sizes of the crystallite nanoparticles that will give a good and higher oil recovery has not been investigated. N.A. Ogolo et al (2010) used 40nm aluminum oxides particles size in their experiment and concluded that the aluminum oxide is the best compared to the other nanoparticles but they failed to provide adequate proof that 40nm is the ideal size [12]. It is therefore essential to study the effect of nanoparticle crystallite sizes in a nanofluid on the interfacial tension of oil for EOR.

CHAPTER 3
METHODOLOGY

3.1 Methodology

The methodology of the work is presented in the following flow chart **(Figure 5)**. It explains the development of the project within time given which are during FYP1 and FYP2 which is 8 months. Thus, this project will be executed as planned in manageable approach in term of time and its feasibility.

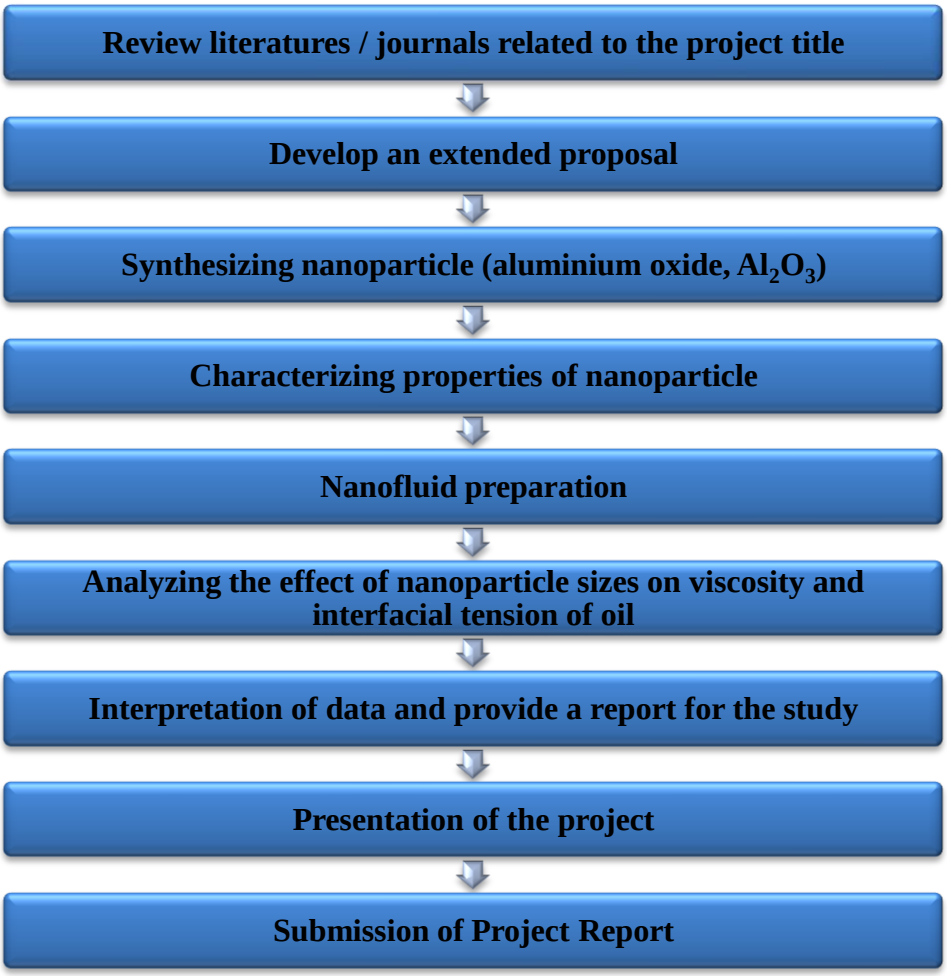

Figure 5: Overall Processes of the Project

3.2 Project Activities

Four major sections will be discussed in this chapter; synthesis and characterization of Al_2O_3, nanofluid preparation and characterization, porous medium properties characterization and the evaluation of recovery by core flooding test.

This project has been divided into two phase. The first phase that will be done during FYP1 is to synthesize the nanoparticle which is the aluminum oxide. There are several synthesis method that can be used such as sol gel synthesis and co-precipitation method. Sol gel method was used to synthesize the Al_2O_3 and annealed at different temperature and result in different nanoparticle sizes. The prepared Al_2O_3 nanoparticles were then characterized using XRD, FESEM, EDX and TEM. The properties such as size and morphology of the nanoparticles will be characterized.

During the second phase, the effect of the nanoparticles on interfacial tension will be analyzed and interpreted as well as the calculation on the oil recovery. This were done during FYP2. Porous medium characterization is conducted using Darcy's Law, permeability, porosity and pore volume are calculated.

3.2.1 Synthesizing Nanoparticles

The nanoparticles used in this project is alumimum oxide (Al_2O_3) nanoparticles. Sol-gel was chosen based on the high chemical homogeneity and purity of the final product, as well as flexibility to manipulate chemical composition, high repeatability and low production cost [17]. Sol-gel method was applied to synthesize the Al_2O_3 particles. Aluminum Nitrate $Al(NO_3)_3$ salt **(Figure 6)** was used as the Al3+ metal ion precursor and nitric acid HNO_3 as the solvents. The solution are then stirred with magnetic stirrer for 2 weeks in order to get a homogenous mixture. The mixture was then stirred for 48 hours at 80°C as shown in **Figure 7** and the resultant gelled mass was dried at 120°C. Dried powder formed was then crushed and grinded and subsequently annealed at 1000°C, 1100°C and 1200°C . The synthesis flow is shown in **Figure 8**. One sample were purchased from Sigma Aldrich with the particle size of 50nm. All the samples are labeled as follow in **Table 1**.

Table 1: Summary of different Al_2O_3 annealed at different temperature

Samples	Label
Al_2O_3 annealed at 1000ºC	Al_2O_3-S1
Al_2O_3 annealed at 1200ºC	Al_2O_3-S2
Al_2O_3 annealed at 1300ºC	Al_2O_3-S3
50nm Al_2O_3 purchased from Sigma Aldrich	Al_2O_3-SA-S4

Figure 6: Aluminium Nitrate Salt, $Al(NO_3)_3$

Figure 7: $Al(NO_3)_3$ with Nitric Acid Stirred with Magnetic Stirrer

Synthesis Flow

Mixing $Al(NO_3)_3$ salt with Nitric Acid
Magnetically stirred to form homogeneous solution
Heating up to 70℃ to obtain milky white gel
Drying gel at 110°C for 72 hours
Grinding the dried powder
Annealing at temperature of 1000°C, 1100°C and 1200°C for 4 hours
Characterization of nanoparticle powder using FESEM, XRD and TEM

Figure 8: Synthesizing of Al_2O_3 by using sol gel method

3.2.2 Characterization of Nanoparticles

The micro structural properties of the nanoparticles e.g. sizes, surface morphology and elemental analysis were conducted by using analytical equipments available in UTP at Centralized Analytical Laboratory (CAL).

3.2.2.1 Field Emission Scanning Electron Microscopy (FESEM)

Supra 55VP Zeiss Variable Pressure Field Emission Scanning Electron Microscope (VP-FESEM) is the electron microscope **(Figure 9).** The VP mode runs the sample chamber at high pressure (20-40Pa) which assisting in charge-compensation of the sample. This allows insulating samples to be analyzed and imaged without coating. Electron microscope has the ability to resolve objects ranging from part of nanometer to micrometer compared to light microscope that has a magnification in the range of 1000 and resolution of 200 nm. When the electron beam interacts with the specimen, it could expose useful information about the sample including its surface morphology and texture, size and shape of the features, composition and crystalline structure.

Figure 9: Supra 55VP Zeiss Variable Pressure Field Emission Scanning Electron Microscope (VP-FESEM)

3.2.2.2 Energy Dispersive X-Ray (EDX)

EDX is linked to the FESEM. EDX is used to indentifies the type of elements present within the sample and quantifies its composition.

3.2.2.3 X-ray Powder Diffraction (XRD)

XRD is used as a characterization tool in identifying the types of phases present in the sample. It is based on the Bragg's equation ($2d \sin \theta = \lambda$) which describes the relation between the angle (θ) and wavelength (λ) of focused x-ray with the distance between atomics, d-spacing (d) in the crystal.

The average particle size, d_{hkl} can be measured using Scherer's Equation 3.1;

$$d_{hkl} = \frac{k\lambda}{\beta_{hkl} \cos \theta} \qquad (3.1)$$

where d_{hkl} is the particle size in nanometers, λ is the wavelength of the radiation, k is a constant equal to 0.89, β_{hkl} is the peak width at half maximum intensity and θ is the peak position.

XRD measurements were conducted using a Bruker A&S D8 Advanced Diffractometer instrument equipped with a CuKα radiation source (λ= 1.5406Å), at 40 kV and 30 mA. The scanning angle (2θ) used was in the range of range of 2–80º at scanning speed and step size of 1.00º/min and 0.05º, respectively. By using EVA software, the resultant spectra were compared with the standard reference to confirm the phase of tested specimen. Information such as Bragg angle (2θ), full width half maximum (FWHM), d-spacing and lattice parameter were also determined using this software.

3.2.2.4 Transmission Electron Microscope (TEM)

TEM offers information on micro texture and nanostructure of electron-transparent specimens. The electron beam passes through the solenoids, down the column, makes contact with the screen where the electrons are converted to light and form an image. During transmission, the speed of electrons directly correlates to electron wavelength; the faster electrons move, the shorter wavelength and the greater the quality and detail of the image. When greater numbers of electrons were able to pass through the specimen, the image form at that particular area will appear lighter, whereby darker areas reflect the dense areas of the specimen. Differences in the brightness provide information on the structure, texture, shape and size of the specimen.

To obtain a TEM analysis, samples need to be sliced thin enough for electrons to pass through, a property known as electron transparency. Few milligrams of nanoparticles were dispersed in 2-propanol and sonicated for about 1 hour. The mixture was then allowed to settle for about 1 hour at room temperature. Two layers consisting of sediment and clear solution were formed. Only few drops of clear solution needed to be dropped on a carbon-coated copper grid. This copper grid was then transferred to a chamber of the TEM. As shown in **(Figure 10)**, TEM used in this research was model Zeiss Libra 200FE for analysis at 200 kV and magnification from 8X to 1,000,000X.

Figure 10: Libra 200FE Zeiss Transmission Electron Microscope

3.2.3 Preparation of Nanofluid

Al_2O_3 nanoparticles were prepared in powder form therefore, they have to be stably suspended in base liquid as from now will be called nanofluids to enable injection into porous medium during core flooding for EOR purpose. Several nanofluid solutions will be prepared by dispersing the Al_2O_3 nanoparticles with the different size in distilled water. A 0.1%wt nanofluid were prepared and further agitated in an ultrasonic bath for 1 hour to reduce nanoparticles agglomeration and ensure long dispersion of Al_2O_3 nanoparticles powder in aqueuous solution.

3.2.4 Crude Oil Characterization

Malaysian Dulang crude oil was used throughout this research. Details of the oil are in **Table 2**. Fluid properties e.g. viscosity and density were measured.

Table 2: Details of the crude oil

Type of Crude	Dulang crude oil
Origin	Malaysia
Density @ 27ºC	0.798 g/cm^2
Viscosity	3cp (Rotational Viscometer)

3.2.5 Oil-aqueous Phase Interfacial Tension Measurement (IFT)

IFT between oil and injection fluids (Al_2O_3 nanofluids and brine) were measured by using Data Physics SVT20N Spinning Drop Video Tensionmeter, equipped with SVTS 20 software package.

The measurement were conducted by controlling the tilt angle and rotation of the oil drop present in the capillary block (**Figure 11**), known as drop phase (phase 1), into excess injection fluids (phase 2) at 6000 rpm. IFT, γ measured in mN/m is calculated based on spinning drop contours according to Laplace-Young method shown in Equation 3.2,

$$\gamma = 2.74156e^{-3}\frac{(\rho_h-\rho_d)\omega^2}{C} \quad (3.2)$$

where ρ_h is the density of the heavy (outer) phase (g/cm3), ρ_d is the density of the light (drop) phase (g/cm3), ω is the rotational velocity (rpm), D is the measured drop width (mm) and C is a coefficient determined by the ratio of the length to the width of the oil drop.

Oil-brine IFT was measured as the reference value for the next reduction in IFT by using other nanofluids. It is important to determine the effect of nanoparticles addition on the recovery efficiency.

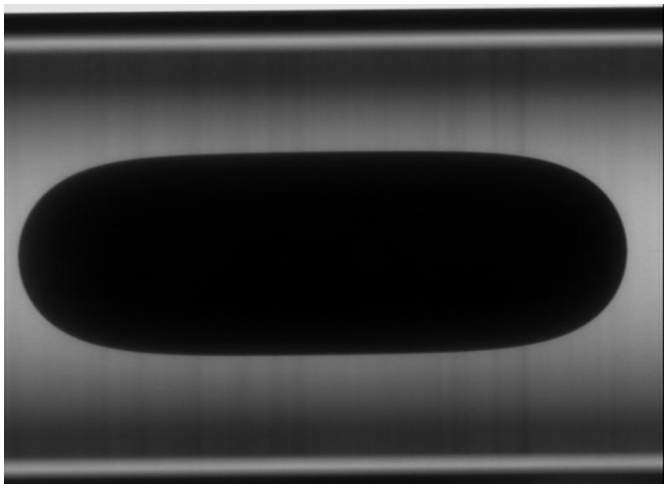

Figure 11: Oil drop present in capillary block

3.3 Core Flooding Experimental Setup

The core flooding experimental setup as shown in **Figure 12** can be classified into three major sections; the injection section, the displacement section and the collection section. Injection section consists of displacement pump, control valve, pressure gauge and injection fluids e.g. brine, oil and nanofluids. All components are connected together by suitable nylon tubing and compatible connectors. Porous medium comprises of silica beads packed in a sealed acrylic column serves as the main component in the displacement section, while measuring cylinders and control valve belong to the collection section. The experiment will be done at surface condition of room temperature at 27ºC and at atmospheric pressure. Surface condition creates one of the worst case scenarios that trigger fine to migrate away from their original position because pressure is very low. High pressure tends to bind the formation grains together. Moreover, a low temperature condition will resulted in high oil viscosity compare to high temperature condition.

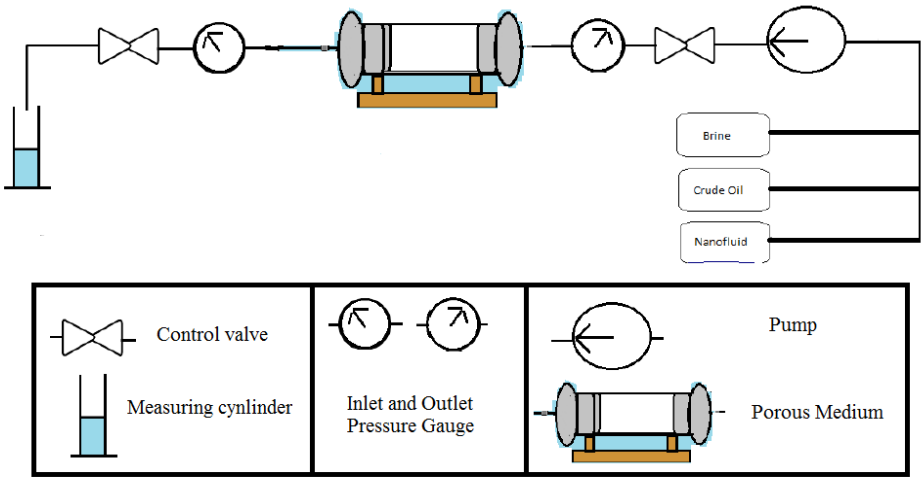

Figure 12: Schematic diagram of core flooding setup

3.4 Reservoir Rocks Characterization

The knowledge of rock and fluid properties are importance to understand the behavior and principles of a reservoir. To determine the properties, laboratory experiment usually conducted on core samples of actual reservoir fluids. In this study, unconsolidated cores made of packed silica beads as a porous medium to replicate the reservoir formation. A 5 cm acrylic tube with diameter of 4.5 cm was used as a column to contain the glass bead with an average mesh size of 30 - 60 μm. The column were then weighed to obtain its dry weight and connected to the pump to enable injection of fluid for example brine injection for the permeability measurement using Darcy's Law. **Figure 13** shows the core setup.

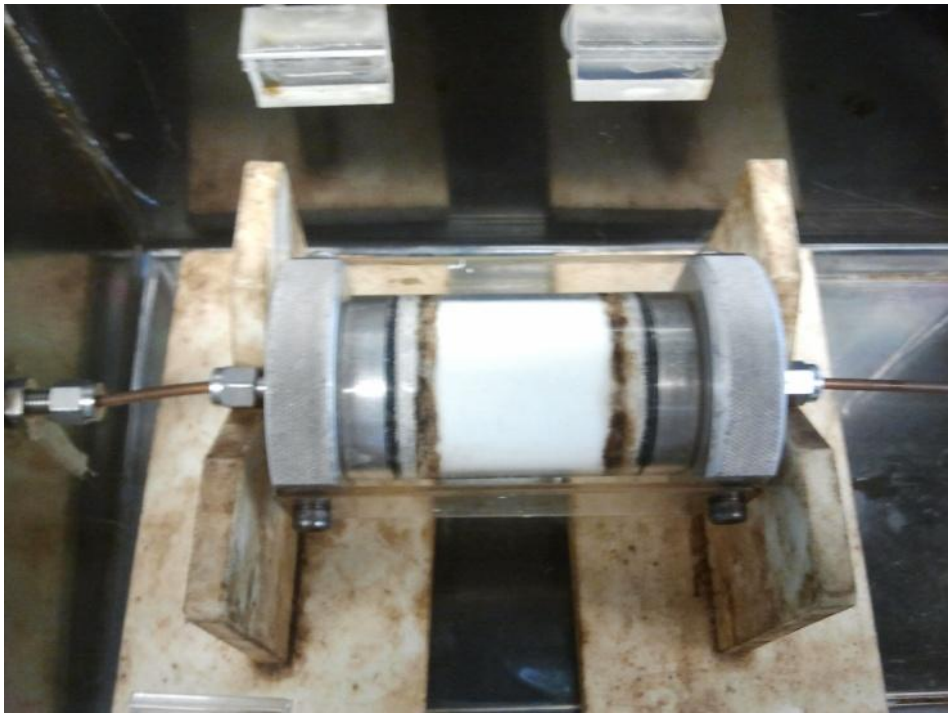

Figure 13: Unconsolidated cores column setup for characterization and coreflooding experiment

3.4.1 Porosity

Porosity is considered as the most important reservoir property. Porosity is the measurement of storage capacity of a reservoir and defined as:

$$\phi = \frac{pore\ volume}{bulk\ volume} \tag{3.3}$$

where ϕ is the porosity usually expressed in term of ratio or percentage. Porosity is divided into two types which are absolute porosity and effective porosity. Absolute porosity is the ration of all pore spaces in the rock to the bulk volume of the rock while effective porosity is the ratio of the interconnected pore spaces to bulk volume of the rock. Effective porosity is the value that is used in all reservoir engineering calculations because it contains fluids that can be produced.

3.4.2 Permeability

Permeability is the ability of a rocks to transmit fluids. High permeability rocks indicate that the rock is permeable and tend to have many large, well connected pores. Permeability can be expressed through Darcy's equation:

$$k = \frac{q\mu}{A}\frac{dL}{dP} \tag{3.4}$$

where k is the permeability, q is the flow rate, μ is the vicosity of the fluids, dL is the length of the rock and dP is the pressure drop as the fluid flow through the porous media.

3.4.3 Fluid Saturation

Oil, water and gas saturations are important parameters in the study of oil and gas reservoirs. Fluid saturations can be defined as the ratio of the volume of fluid in a core to the pore volume of the sample and expressed by:

$$Fluid\ Saturation = \frac{Total\ volume\ of\ the\ fluid}{Pore\ Volume} \tag{3.5}$$

By applying the above concept, saturation of each reservoir oil and water only gives,

$$S_o = \frac{Volume\ of\ Oil}{Pore\ Volume} \tag{3.6}$$

$$S_w = \frac{Volume\ of\ Water}{Pore\ Volume} \tag{3.7}$$

where So and Sw are the saturation value of the oil and water respectively. The saturation of each individual phase ranges between zeros to 100 percent. By definition, the sum of the saturations is 100%, therefore,

$$S_o + S_w = 1.0 \tag{3.8}$$

3.5 Core Flooding Tests

In the core flooding test, distilled water (as controlled set of experiment) and Al_2O_3 nanofluid are used as the injecting fluid for EOR. The experiment will be carried out at surface condition at room temperature and at atmospheric pressure. This is because surface condition creates one of the worst case scenarios that trigger

fine particles to migrate away from their original position because pressure is very low. High pressure tends to bind the formation grains together. Moreover, a low temperature condition will resulted in high oil viscosity compare to high temperature condition.

The reservoir material will be prepared by saturating glass beads by continuous injection of brine at the concentration of 36,000 ppm at rate of 1ml/min to achieve base permeability which creates a condition where differential pressure between inlet and outlet becomes stable. Then Dulang crude oil having dynamic viscosity of 3cp at room temperature was injected at the rate of 0.8/min into the porous medium to flush out brine until oil emerged from the outlet. This step is to ensure that pore spaces are filled with oil and amount of oil contain in the porous medium can be determined.

Next, water flooding process will be done by continuously injecting brine of 36,000 ppm at 1ml/min to replicate the secondary recovery stage. In estimate 50% of the OOIP will be displaced out before leaving the remaining oil to be recovered in the next stage.

For EOR stage, 4 pore volume of 0.1 wt% concentration of nanofluids were injected at a rate of 1.0ml/min. Distilled water acts as a controlled experiment and therefore the recovery obtained by injecting distilled water will be the reference value for the nanofluids injection. The injection of EOR fluids were stopped when there is no more oil to produce. E_R was calculated using the volume of oil recovered in EOR stage as a percentage of the oil present after water flooding, remaining oil in place (ROIP), as presented by Equation :

$$E_R\ (\%ROIP) = \left(\frac{Volume\ of\ oil\ recovered\ in\ EOR\ fluid\ injection}{Volume\ of\ ROIP}\right) x100 \quad (3.9)$$

3.6 Key Milestone

Below are the key milestones that need to be achieved throughout the period of the project which is approximately 29 weeks.

Milestone	Week
Early Project Development Stage • Research background • Scope of studies and Assumptions • Literature review	1 - 8
Middle Project Development Stage • Detailed research • Synthesizing nanoparticles • Nanofluid preparation • Conducting core flooding	9 - 21
Final Stage • Results gathering • Analyzing the sizes of nanoparticles on EOR • Completing the documentation	22 - 29

3.7 Gantt Chart

No.	Task Activities	Weeks																												
		FYP1														FYP2														
		1	2	3	4	5	6	7	8	9	10	11	12	13	14	15	16	17	18	19	20	21	22	23	24	25	26	27	28	29
1	Consolidation of FYP Topics																													
2	Selection of Project Topic																													
3	Preliminary Research Work																													
4	Preparation for Extended Proposal																													
5	Submission of Extended Proposal																													
6	Proposal Defence																													
7	Project Work Continues																													
	- synthesizing nanoparticle																													
	- characterizing nanoparticles properties																													
8	Submission of Interim Draft Report																													
9	Submission of Interim Report																													
10	Project Work Continues																													
	- forming nanofluid																													
	- conducting coreflooding and analyzing the result																													
11	Submission of Progress Report																													
12	Project Work Continues																													
	- interpretation of data																													
13	Pre-SEDEX																													
14	Submission of Draft Report																													
15	Submission of Dissertation																													
16	Submission of Technical Paper																													
17	Oral Presentation																													
18	Submission of Project Dissertation																													

CHAPTER 4
RESULTS AND DISCUSSIONS

4.1 Characterization of aluminum oxide nanoparticles

Three samples of of Al_2O_3 were annealed at 1000ºC**,** 1100ºC and 1200ºC. The annealing processes for all samples were conducted for 4 hours at same heating and cooling rate which is 10ºC/min, at holding temperature ranging from 1000ºC to 1200ºC**.**

4.1.1 Field Emission Scanning Electron Microscopy (FESEM)

FESEM images of Al_2O_3 nanoparticles are shown in **Figure 14**. Annealed at ranging temperature of 1000ºC to 1200ºC, homogenous fibrous pore network of nanoparticles could be observed on the surface in throughout the sample. Distinct grain boundaries formed to give spherical features of dimensions around 190nm to 340 nm particle size as shown in **Figure 14(c)**. Jones et al (2007) also concluded almost similar results and predicted that this phenomenon was attributed to the smaller particles being sintered together causing a collapse in the small pores resulting in the formation of larger, less dense pores [19].

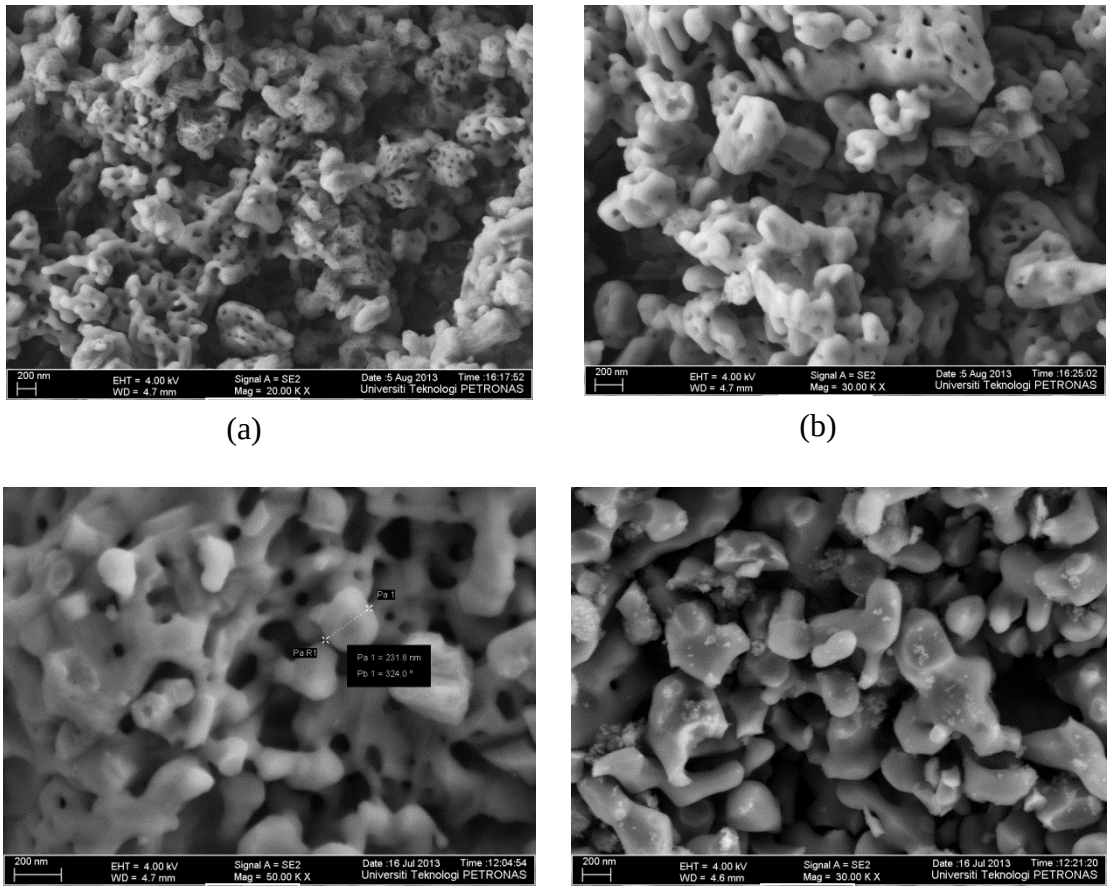

Figure 14: FESEM images for Al_2O_3 annealed at temperature of (a) 1000ºC, (b) 1100ºC and (c) 1200ºC . (d) FESEM image for Al_2O_3 purchased from Sigma Aldrich

From the FESEM images result, all the samples particle sizes can be summarized in the **Table 3.** The result shows that the particle sizes of all the samples are slightly the same.

Table 3: Summary of Al_2O_3 particle size

Sample Label	Particle Size, nm
Al_2O_3-S1	180 - 300
Al_2O_3-S2	190 - 330
Al_2O_3-S3	190 - 340
Al_2O_3-SA-S4	220 - 350

4.1.2 Energy Dispersive X-Ray (EDX)

Elemental composition of the samples was identified from EDX analysis by using OXFORD INCA X-ray Microanalysis system. The atomic and weight percentages of these elements are tabulate in **Table 4**. From the EDX analysis, presence of aluminum and oxygen atoms is evident by the relative abundance of each of the element which is comparable to the theoretical stoichiometric values. It can be concluded that Al_2O_3 nanoparticles produced were of high purity when it is annealed at 1200°C. The percentage weight difference,% is contributed to the presence of impurities derived from starting materials and metal ions having a different melting temperature [18]. Aluminum to oxygen atoms ratio should be kept 2:3 based on the chemical formula, however from the elemental analysis, a slight deviation in the atomic percentage was observed. Standard atomic weight of oxygen atom is 15.9994g/mol and 26.9815g/mol for aluminum. From this EDX analysis, it can be concluded that annealing temperature higher than 1100°C is required to sufficiently remove residual water and impurities.

Table 4: Comparison of weight and atomic ratio from EDX analysis of Al_2O_3 nanoparticles

Sample	Element	Measured Weight Ratio (%)	Standard Atomic Weight (g/mol)	Theoretical Weight Ratio (%)	Percentage Difference (%)	Measured Atomic Ration (%)	Theoretical Atomic Ratio (%)	Percentage Difference (%)
Al_2O_3-S3	O	46.54	15.9994	47.07	-1.08	59.48	60	-0.87
	Al	53.46	26.9815	52.93	1.00	40.52	40	1.30
Al_2O_3-SA-S4	O	45.35	15.9994	47.07	-3.65	58.33	60	-2.78
	Al	54.65	26.9815	52.93	3.25	41.67	40	4.18

4.1.3 X-Ray Diffraction (XRD)

XRD patterns for Al_2O_3 nanoparticles at three different temperatures are shown in **Figure 15.** It can be seen that Al_2O_3 peaks have become better defined as the annealing temperature increased. Sharbatdaran M. et al (2009) conclude that annealing temperature does play a significant role of improving the cristallinity of final product[20]. Sharper peaks with increasing annealed temperature indicate that the enhancement of crystallinity.

Lattice parameters of Al_2O_3 calcined at different temperature are summarized in **Table 5.** From the table it can be observed that there was little change in lattice parameters when the annealing temperature was increased. The changing in lattice parameters can be contributed to the change of particle size and quantum size[21].

Table 5: Lattice parameters Al_2O_3 prepared at 1000°C, 1100°C and 1200°C

X-Ray Diffraction						
Samples	Standard Reference Card No. (SS-NNNN)	Wavelength	System	Lattice parameter		
				a	b	c
1000	11-0661 (D)	1.5406	Hexagonal (Rh)	4.759	4.759	12.991
1100	02-1227 (D)	1.5406	Hexagonal (Rh)	4.749	4.749	12.965
1200	43-1484 (D)	1.5406	Hexagonal (Rh)	4.759	4.759	12.992

In determining the crystallite size of nanoparticles, TEM is the best way, however, XRD is also widely used. The average crystallite size is calculated using Scherer's equation 3.1. The crystallite size of the prepared sample are summarized in **Table 6.**

Table 6: Crystallite size of Al_2O_3 using Scherer's equation

Temperature	k	λ	FWHM	β	2-THETA	θ	cos	crystallite size	
								(m)	nm
1000°C	0.89	1.5406E-10	0.5	0.008727778	43.3	21.65	0.93	1.68925E-08	16.9
1100°C	0.89	1.5406E-10	0.3	0.005236667	43.3	21.65	0.930	2.81541E-08	28.2
1200°C	0.89	1.5406E-10	0.2	0.003491111	43.3	21.65	0.930	4.22312E-08	42.2

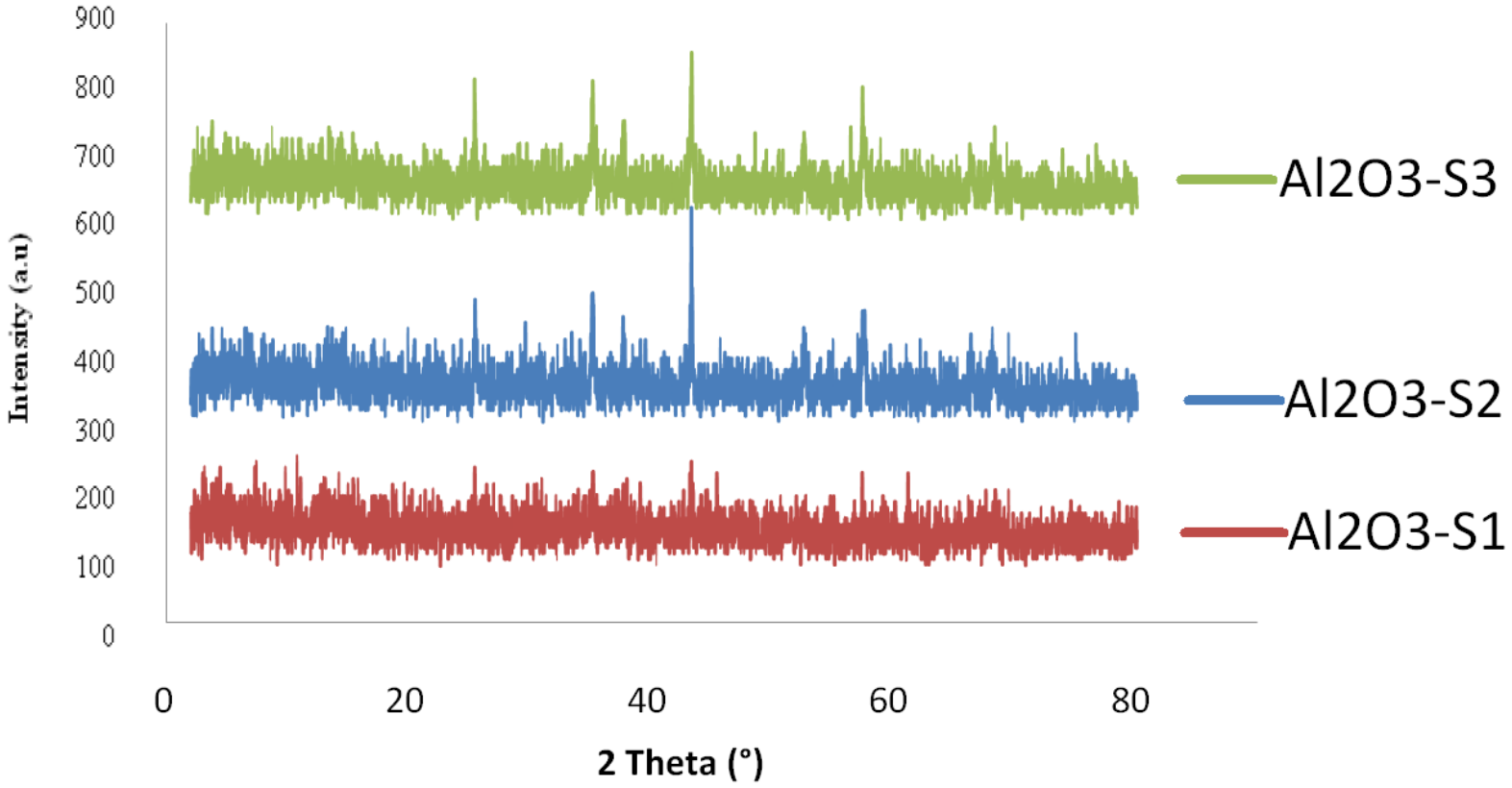

Figure 15: XRD pattern for Al_2O_3 of different samples which annealed at temperature of 1000ºC, 1100ºC and 1200ºC

4.1.4 Transmission Electron Microscope (TEM)

TEM micrographs shown in **Figure 16** gives the images of the synthesized Al_2O_3 nanoparticles crystallite size and shape. Since Al_2O_3 nanoparticles was severely agglomerated in iso-propanol, identification of the morphology and particle size could not accurately done. Based on **Figure 16**, image of crystal having hexagonal shape can be observed. Crystallite size from TEM can be used to compare with the crystallite size calculated using Scherer method form XRD analysis. A. Khorsand Zak et al (2011) state that there was a 25% variation between the TEM and XRD results for particles size. This is because strain applied on the atoms surface due to surface effect are not considered in XRD measurements [22].

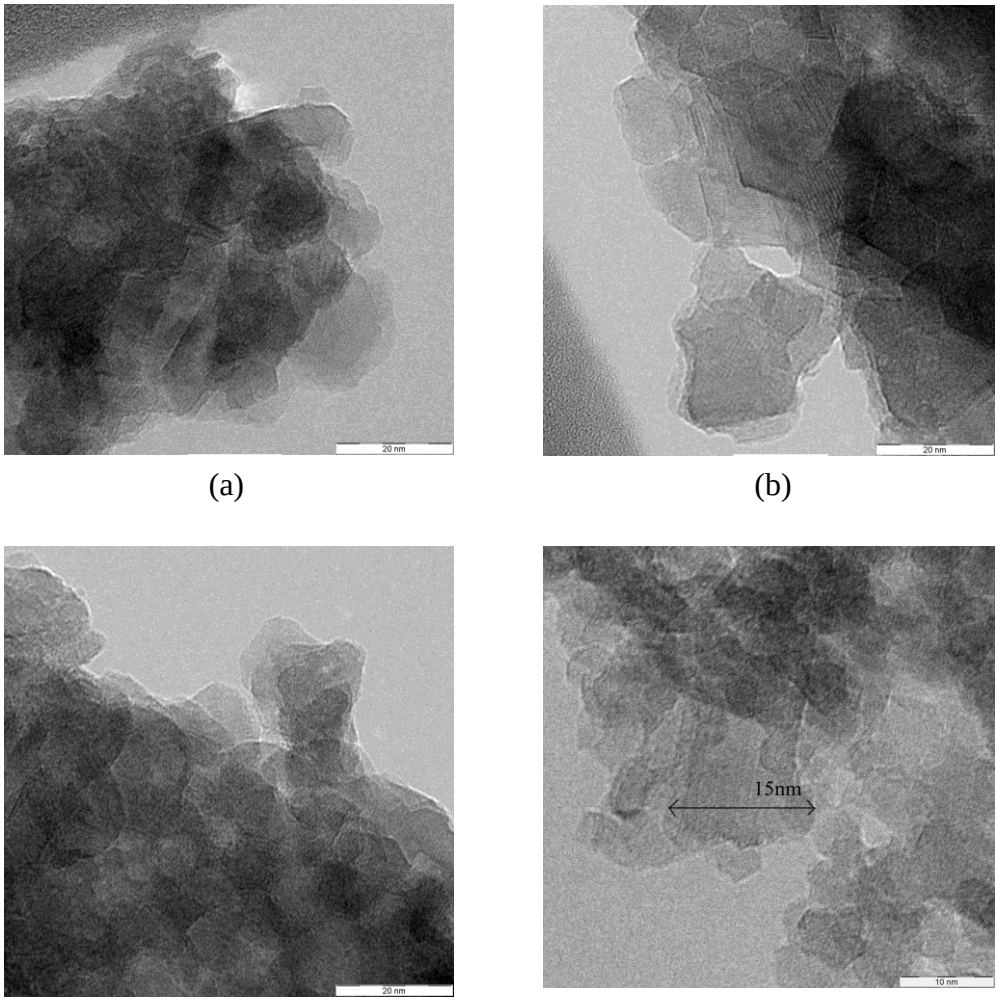

(a) (b)

(c) (d)

Figure 16: TEM micrographs imaging for Al_2O_3 annealed at temperature of (a) 1000ºC, (b) 1100ºC and (c) 1200ºC . (d) TEM micrograph for Al_2O_3 purchased from Sigma Aldrich

4.1.5 Al_2O_3 nanoparticles crystallite size

After all the samples have been characterized using XRD, FESEM, EDX and TEM, Al_2O_3 nanoparticles crystallite size can be summarized in the **Table 7.**

Table 7: Summary of Al_2O_3 crystallite size

Sample Label	Crytallite size
Al_2O_3-S1	14-18nm
Al_2O_3-S2	20-30nm
Al_2O_3-S3	40-45nm
Al_2O_3-SA-S4	±20nm

4.2 Interfacial tension (IFT) measurement

Interfacial tension values between crude oil and various injection fluids containing nanoparticles and surfactant were measured and compared, as presented in **Table 8**. There were five types of fluids involved in the measurement which are brine and 4 different sizes of Al_2O_3 nanoparticle in nanofluid. Initially, oil-brine IFT value was measured as 20.299 mN/m, almost in the range of typical oil-brine IFT, which is around 20-50 mN/m. When 0.1 wt% of Al_2O_3 nanofluid is in contact with the crude oil, the IFT value was tremendously decreased as shown in **Figure 17.**

Initially, oil-brine IFT value was measured at 20 mN/m which is in the range of typical oil-brine IFT of 20-50 mN/m[23]. When 0.1 wt% of Al_2O_3 nanofluid of different particles size for example sample Al_2O_3-S1 is in contact with the crude oil, the IFT value decrease to 8 mN/m as refer to **Figure 17**. This is because, when the Al_2O_3 molecules are absorbed at the interface, their hydrophobic tails will reside on the non-polar phase, and their hydrophilic head preferentially, oriented towards the aqueous solution, lead to reduction of IFT [24].

From the **Figure 17,** it can be observed that as the nanoparticle sizes increase, the IFT values is slightly increase. Cigdem O. Metin et al (2012) states that a decrease in IFT is observed as particle size decreases at a given nanoparticle concentration [25].

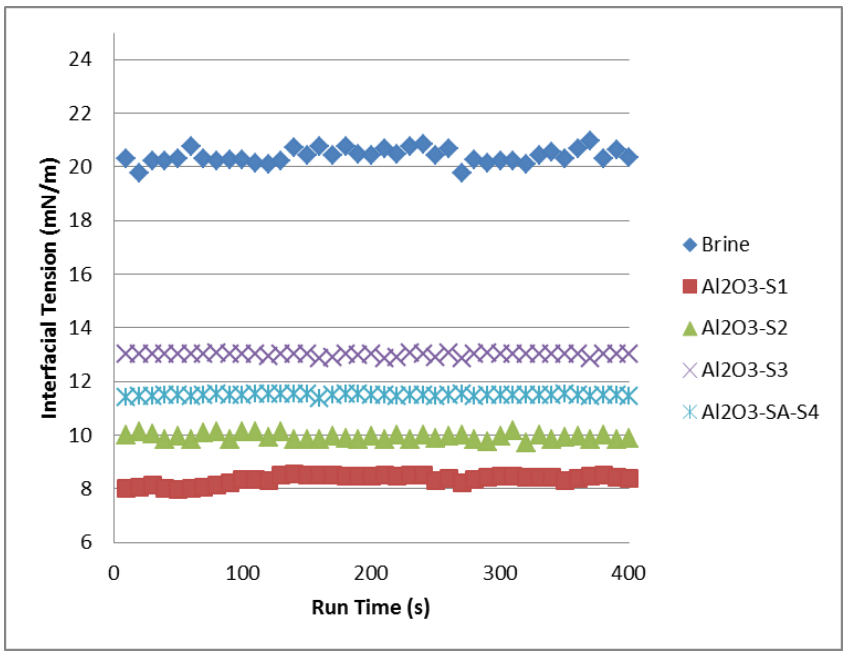

Figure 17: Dynamic IFT measurement of the injection fluids

Table 8: Dynamic interfacial tension value between crude oil and injection fluids

Time (s)	Brine	Al_2O_3-S1	Al_2O_3-S2	Al_2O_3-S3	Al_2O_3-SA-S4
10	20.299	8.013	9.999	13.031	11.432
20	19.789	8.054	10.143	13.028	11.462
30	20.209	8.134	10.044	13.018	11.452
40	20.226	8.035	9.848	13.041	11.494
50	20.307	7.988	9.982	13.026	11.480
60	20.751	8.026	9.837	13.026	11.468
70	20.301	8.05	10.095	13.023	11.514
80	20.243	8.124	10.129	13.048	11.522
90	20.271	8.237	9.843	13.022	11.512
100	20.251	8.338	10.124	13.021	11.482
110	20.131	8.334	10.132	13.02	11.540
120	20.12	8.312	9.913	12.956	11.521
130	20.226	8.521	10.12	13.031	11.538
140	20.719	8.538	9.841	13.021	11.517
150	20.417	8.527	9.851	13.038	11.527
160	20.758	8.522	9.857	12.87	11.361
170	20.426	8.503	9.957	12.892	11.482
180	20.751	8.493	9.862	13.02	11.522
190	20.461	8.48	9.855	12.966	11.534
200	20.417	8.46	9.975	13.04	11.503
210	20.683	8.496	9.857	12.871	11.496
220	20.464	8.474	9.987	12.894	11.460
230	20.761	8.518	9.858	13.048	11.496
240	20.833	8.522	9.996	13.03	11.480
250	20.43	8.32	9.865	12.917	11.474
260	20.677	8.381	9.977	13.058	11.506
270	19.789	8.217	9.997	12.858	11.518
280	20.285	8.346	9.858	13.012	11.474
290	20.131	8.437	9.776	13.048	11.511
300	20.245	8.477	9.983	13.044	11.492
310	20.245	8.468	10.175	13.019	11.514
320	20.095	8.452	9.702	13.012	11.485
330	20.452	8.421	9.999	13.042	11.493
340	20.564	8.416	9.848	13.018	11.509
350	20.324	8.312	9.941	13.014	11.525
360	20.687	8.383	9.968	13.026	11.480
370	20.954	8.456	9.852	12.859	11.437
380	20.321	8.501	9.986	13.014	11.477
390	20.658	8.423	9.856	13.023	11.478
400	20.354	8.387	9.861	13.013	11.470

4.3 Reservoir rock properties

Permeability and porosity of the porous medium which consist of unconsolidated silica beads were measured.

Table 9:Permeablity and porosity of the porous medium

Permeability	Porosity (%)
1250 mD	38

The porous medium is highly permeable with an average permeability of 1250 mD which can be conclude as an unconsolidated formation. As the experiment is conducted at surface condition, the low pressure condition has contribute to grain migration and the grain is not bind together which lead to high permeability.

4.4 Effect of nanoparticle sizes injection for oil recovery

In the core flooding test, distilled water (as controlled set of experiment) and 0.1 wt% Al_2O_3 nanofluids are used as the injecting fluid for EOR.

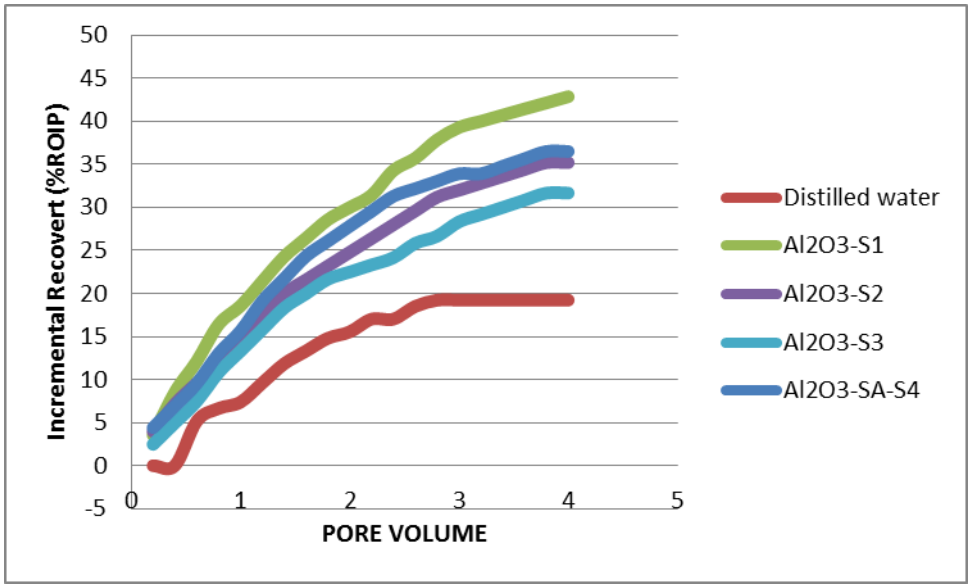

Figure 18: Comparison of the incremental recovery versus pore volume injected Al_2O_3 nanofluids

Based on **Figure 18, a**fter 4 PV of Al_2O_3 nanofluids injection, it can observed that Al_2O_3 nanofluids with different in Al_2O_3 nanoparticle sizes will produce at different incremental recovery. Smaller particle size which is sample label Al_2O_3-S1 (14-18nm) gives the highest recovery of 43% as compared to bigger particle size. The distilled water which is used as a control set of injecting fluid only produce at recovery of 19%.

The relationship between IFT value and oil recovery is presented in **Figure 19.**

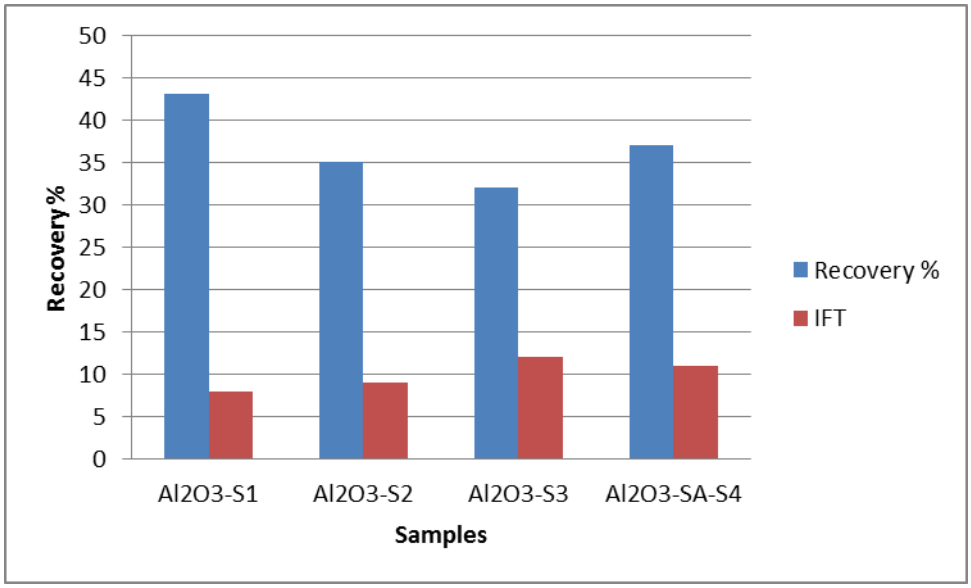

Figure 19: Relationship between the IFT and oil recovery

Based on **Figure 19** we can conclude that the oil recovery is inversely proportional to IFT value. As the IFT value is decreased, the oil recovery will be increased. Well design surfactants as for this study is the nanofluids will create micro emulsions at the interface between crude oil and water, thus reducing the IFT value, which consequently will mobilize the residual oil and result in improved oil recovery [26].

CHAPTER 5
CONCLUSIONS

5.1 Conclusion

It is proven that nanoparticles dispersed in nanofluids can be used as an EOR method to recover oil from the reservoir.

The objective of this study is achieved by:

1. Successfully synthesized high crstallinity of hexagonal Al_2O_3 nanoparticles having average crystallite size of 14-18nm, 20-30nm and 40-45nm with impurities levels below 10%.
2. When smaller Al_2O_3 nanoparticles (Al_2O_3-S1 size of 14-18nm) is dispersed in nanofluid and is in contact with the crude oil, the IFT between the two fluids is decreases the most as compared to bigger nanoparticle sizes.
3. From core flooding tests, highest recovery by Al_2O_3 nanofluids is achieved in Al_2O_3 nanoparticles crystallite size of 14-18nm (smallest as compared to other Al_2O_3 nanoparticles used in this study) which gives recovery of 43% ROIP.
4. Improved in oil recovery is affected by the crystallite size of the nanoparticle and not from the particle size. From the FESEM images, we can conclude that all the samples are having the same ranging particle size of 180 - 350, which mean that the increase in the oil recovery is not affected by the particle size.

5.2 Recommendation

Up to now, this EOR method has been successfully demonstrated and give a positive results for further development. Few recommendations for future work are being listed below, in order to ensure a good achievement and feasibility of this method, before it is put into practice in the field.

1. Feasibility in HTHP condition

   Core flooding test should be conducted in high temperature and pressure system as to confirm the applicability of this method to be used in HTHP environment.

2. Nanoparticles morphology

   The effect of nanoparticles morphology on the oil recovery also need to be studied as different morphology will give a different result and the best morphology should be used for optimum oil recovery.

REFERENCES

[1] Dong, H., Hong, Y., Weng, R.: (Sept. 2006 'The Effect of Wettability on Oil Recovery of Alkaline/Surfactant/Polymer and Polymer Flooding', SPE 102564, Texas USA. Pp. 1 - 8.

[2] U.S. Energy Information Administration (EIA),"International Energy Outlook 2013 With Projections to 2040", July 2013, Washington, DC 20585.

[3] U.S. Energy Information Administration (EIA),"The Annual Energy Review 2011(AER)", September 2012, Washington, DC 20585.

[4] Aleklett, K., Hook, M. & Jakobsson, K. (2010). The Peak of the Oil Age – Analyzing The World Oil Production Reference Scenario in World Energy Outlook 2008. Energy Policy, 38(3), 1398–1414.

[5] Lakatos, I, & Szabó, J. L. (2009, June 8-11). Role of conventional and unconventional hydrocarbons in the 21st century: Comparison of resources, reserves, recovery factors and technologies. Paper presented at the SPE/EUROPEC/EAGE Annual Conference and Exhibition, Amsterdam, The Netherlands.

[6] Sandrea, I. & Sandrea, R (2007). Global Oil Reserves – Recovery Factors Leave Vast Target for EOR Technologies. *Oil and Gas Journal, 105*(41), 44-48.

[7] Mai, A. & Kantzas, A. (2007). Heavy Oil Waterflooding: Effects of Flow Rate and Oil Viscosity. *Journal of Canadian Petroleum Technology, 48*(3), 42-51.

[8] Thomas, S. (2007). Enhanced Oil Recovery - An Overview. Canada: Institu Francais du Petrole.

[9] Lake, L., Schmidt, R. and Venuto, P.: 1992 "A niche for enhanced oil recovery in 1990's", Oilfield Review, 55 - 61.

[10] M. Abtahi and O. Torsaeter, "Experimental Reservoir Engineering - Laboratory Wokbook" 6-32

[11] Onyekonwu, M. O. and Ogolo, N. A., (AUG. 2010), 'Investigating the Use of Nanoparticles in Enhancing Oil Recovery', SPE 140744, Rivers State, Nigeria. Pp. 1 - 13.

[12] N.A. Ogolo, O.A. Olafuyi, and M.O. Onyekonwu: (April 2012) 'Enhanced Oil Recovery Using Nanoparticles', SPE 160847, Al-Khobar, Saudi Arabia. Pp. 1 - 9.

[13] Y.Dandekar, A. (2006). *Petroleum Reservoir Rock and Fluid Properties.* USA: Taylor & Francis Group.

[14] M. Dong, H. Z. (2010). Which one is more important in chemcial flooding for enhanced oil recovery,lowering interfacial tension or reducing oil permeability. *Energy Fuels*, 1829-1836.

[15] Wasan, D. T. and Nikolov, A. D., (2003), 'Spreading of Nanofluids on Solids', Nature, 423: 156 - 159.

[16] Luky Hendraningrat, L. S. (2012). A Glass micromodel Experimenal Study of Hydrophilic Nanoparticles Retention for EOR Project. *SPE 159161*.

[17] Ting Ke Tseng, Yi shing lin, Yi Ju Chen and Hsin Chu (2010), "A Review of Photocatalysts Prepared by Sol-Gel Method for VOCs Removal", International Journal of Molecular Sciences ISSN 1422-0067

[18] Kumar, V. R., Kavitha, V. T., Wariar, P. R. S., Nair, S. U. K., Koshy, J (2011). Characterization, sintering and dielectric properties of nanocrystalline zinc oxide prepared by a citric acid-based combustion route. Journal of Physics and Chemistry of Solids, 72(4), 290-293.

[19] Jones, C. D., Barron, A. R. (2007). Porosity, crystal phase, and morphology of nanoparticle derived alumina as a function of the nanoparticle's carboxylate substituent.. Materials Chemistry and Physics, 104(2-3), 460-471.

[20] Sharbatdaran, M., Amini, M. M., & Maj, A. (2010). Effect of aluminium alkoxide with donor-functionalized group on texture and morphology of the alumina prepared by sol–gel processings. *Materials Letters, 64(*4), 503-505.

[21] M. Hosokawa, K. Nogi, M. Naito, T. Yokoyama, Nanoparticle Technology Handbook, Elsevier, Amsterdam, 2007.

[22] Khorsand Zak, A., Ebrahimizadeh Abrishami, M., Abd. Majid, W.H., Yousefi, R., Hosseini, S.M. (2011). Effects of annealing temperature on some structural and optical properties of ZnO nanoparticles prepared by a modified sol–gel combustion method. Ceramics International, 2011, 37, 393-398.

[23] Bera, A., Ojha, K., Mandal, A., Kumar, T. (2011). Interfacial tension and phase behavior of surfactant-oil-brine system. *Colloids and Surfaces A: Physicochem. Eng. Aspects, 383*(1-3), 114-119.

[24] Singh, P. K., Anoop, K. B., Patel, H. E.., Sundararajan, T., Pradeep, T., Das, S. K. (2010). Anomalous Size Dependent Rheological Behavior of Alumina Based Nanofluids. *International Journal of Micro-Nano Scale Transport, 1(*2), 179-188.

[25] Cigdem O. Metin,1 Jimmie R. Baran, Jr.,2 and Quoc P. Nguyencor (2012), "Adsorption of surface functionalized silica nanoparticles onto mineral surfaces and decane/water interface", J Nanopart Res. 2012 November; 14(11): 1246.

[26] Sara Bülow Sandersen, 2012, Enhanced Oil Recovery with Surfactant Flooding Ph.D. Thesis, Department of Chemical and Biochemical Engineering Technical University of Denmarkb Kongens Lyngby, Denmark

[27] H.R Nares, P Schacht Hernandez, M.A. Ramirez Garnica, and M.C. Cabrera Reyes (2007) "Heavy-Crude-Oil Upgrading With Transition Metals". SPE 107837, Buenos Aires, Argentina.

[28] Bjornar Engeset, 2012, "The Potential of Hydrophilic Silica Nanoparticles for EOR Purposes", Ph.D. Thesis, Department of Petroleum Engineering and Applied Geophysics Norwegian university of Science and Technology.

[29] China Oilfield Technology Services Group Limited, 2007 <http://www.chinaoilfieldtech.com/oilrecovery.html>.

APPENDIX A

XRD DATA

1. Crystallographic properties of aluminium oxide nanoparticles annealed at various temperature.

a) sample **Al_2O_3 -S1**

SS-NNNN	Formula	Y-Scale	d x by	Waveleng	System	Volume
11-0661 (D	alpha-Al2(	50	1	1.5406	Hexagona	254.803

a	b	c	alpha	beta	gamma	Bravais L.	Space Gro
4.759	4.759	12.991	90	90	120	Primitive	R-3c (167)

Sample Name	Left Angle	Right Angle	Left Int.	Right Int.	Obs. Max
	2-Theta °	2-Theta °	Cps	Cps	2-Theta °
Al2O3-annealed at 1000	42.9	43.6	5.13	5.16	43.2

d (Obs. Max)	Max Int.	Net Height	FWHM	Chord Mid.	I. Breadth	Gravity C.
Angstrom	Cps	Cps	2-Theta °	2-Theta °	2-Theta °	2-Theta °
2.09158	6.05	0.91	0.5	43.3	0.5	43.3

d (Gravity C.)	Raw Area	Net Area
Angstrom	Cps x 2-Theta °	Cps x 2-Theta °
2.08917	3.828	0.434

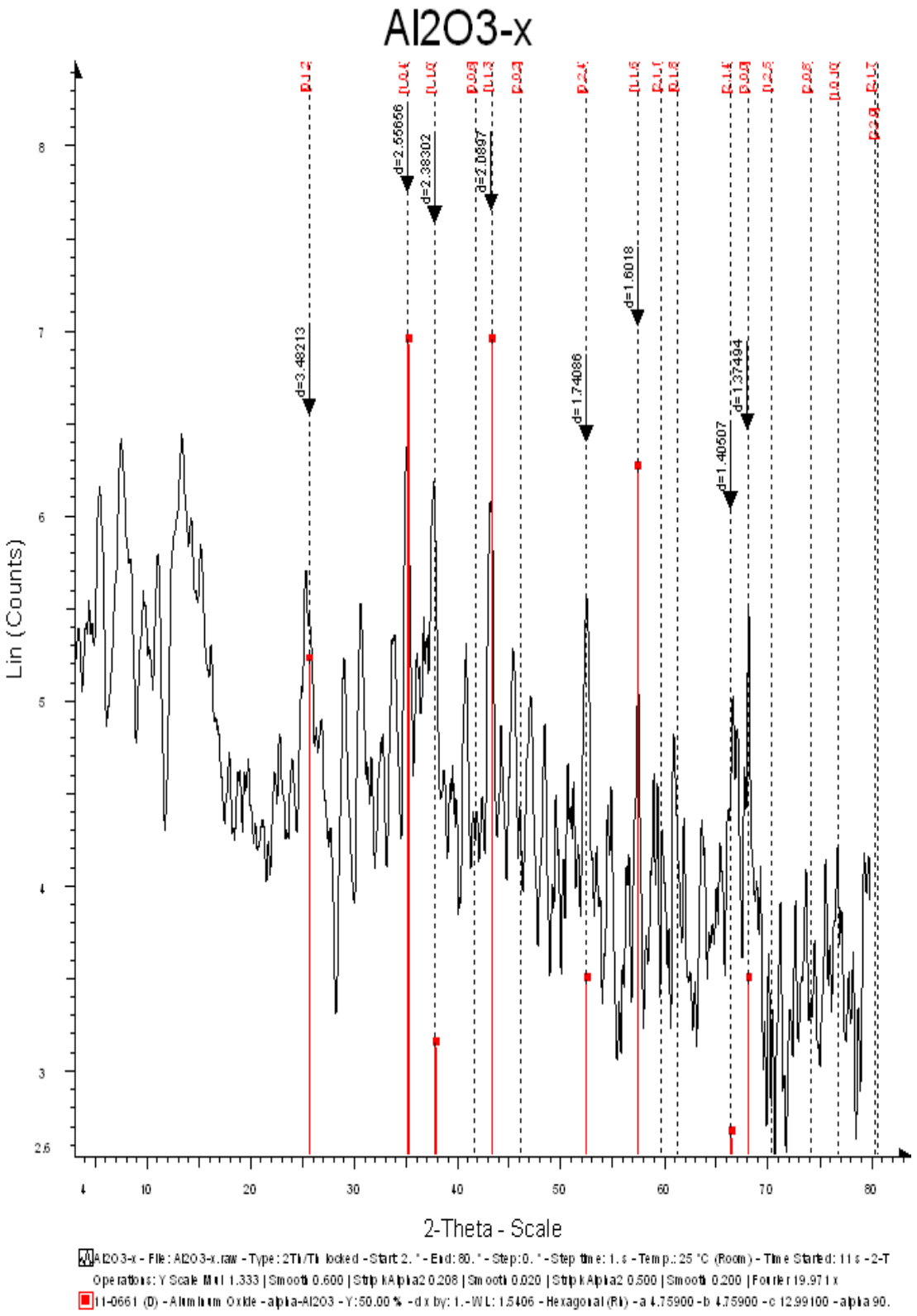

Figure 1 (a): XRD diffraction pattern of Al_2O_3 annealed at 1000°C

b) Sample **Al_2O_3 -S2**

SS-NNNN	Formula	Y-Scale	d x by	Wavelength	System	Volume
02-1227 (D)	alpha-Al2O3	50	1	1.5406	Hexagonal (Rh)	253.226

a	b	c	alpha	beta	gamma	Bravais L.	Space Group
4.749	4.749	12.965	90	90	120	Primitive	R-3c (167)

Sample Name	Left Angle	Right Angle	Left Int.	Right Int.	Obs. Max
	2-Theta °	2-Theta °	Cps	Cps	2-Theta °
Al2O3-1100	43.1	43.6	7.21	3.35	43.3

d (Obs. Max)	Max Int.	Net Height	FWHM	Chord Mid.	I. Breadth
Angstrom	Cps	Cps	2-Theta °	2-Theta °	2-Theta °
2.08894	11.1	5.36	0.3	43.3	0.3

Gravity C.	d (Gravity C.)	Raw Area	Net Area
2-Theta °	Angstrom	Cps x 2-Theta °	Cps x 2-Theta °
43.3	2.08714	4.16	1.621

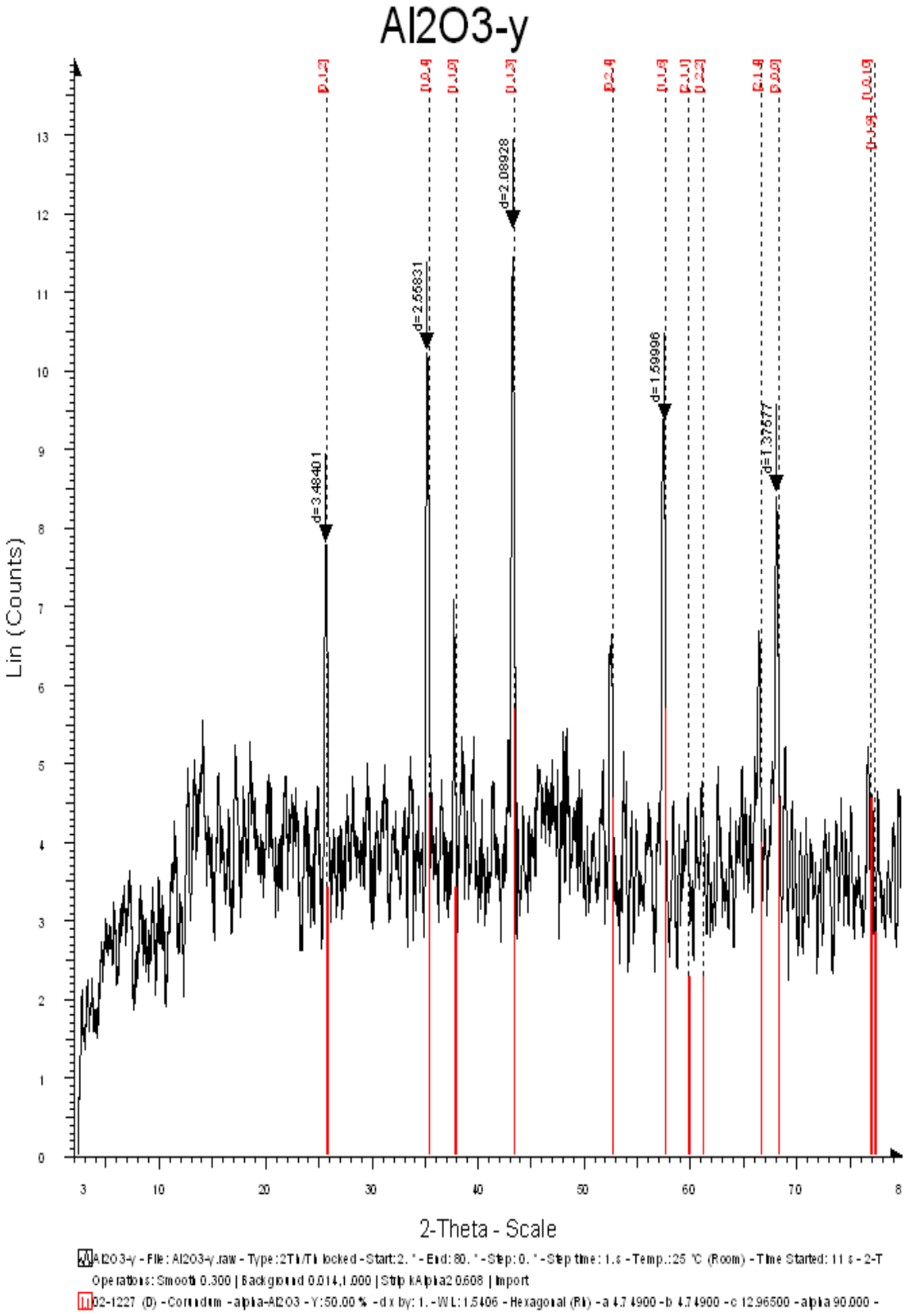

Figure 1(b): XRD diffraction pattern of Al_2O_3 annealed at 1100°C

c) Sample **Al_2O_3 -S3**

SS-NNNN	Formula	Y-Scale	d x by	Wavelength	System	Volume
43-1484 (D)	Al2O3	50	1	1.5406	Hexagonal (Rh)	254.844

a	b	c	alpha	beta	gamma	Bravais L.	Space Group
4.7592	4.7592	12.992	90	90	120	Primitive	R-3c (167)

Sample Name	Left Angle	Right Angle	Left Int.	Right Int.	Obs. Max
	2-Theta °	2-Theta °	Cps	Cps	2-Theta °
Al2O3-1200	43.2	43.5	9.67	1.26	43.3

d (Obs. Max)	Max Int.	Net Height	FWHM	Chord Mid.	I. Breadth
Angstrom	Cps	Cps	2-Theta °	2-Theta °	2-Theta °
2.0869	13.8	6.81	0.2	43.4	0.2

Gravity C.	d (Gravity C.)	Raw Area	Net Area
2-Theta °	Angstrom	Cps x 2-Theta °	Cps x 2-Theta °
43.4	2.08527	3.101	1.352

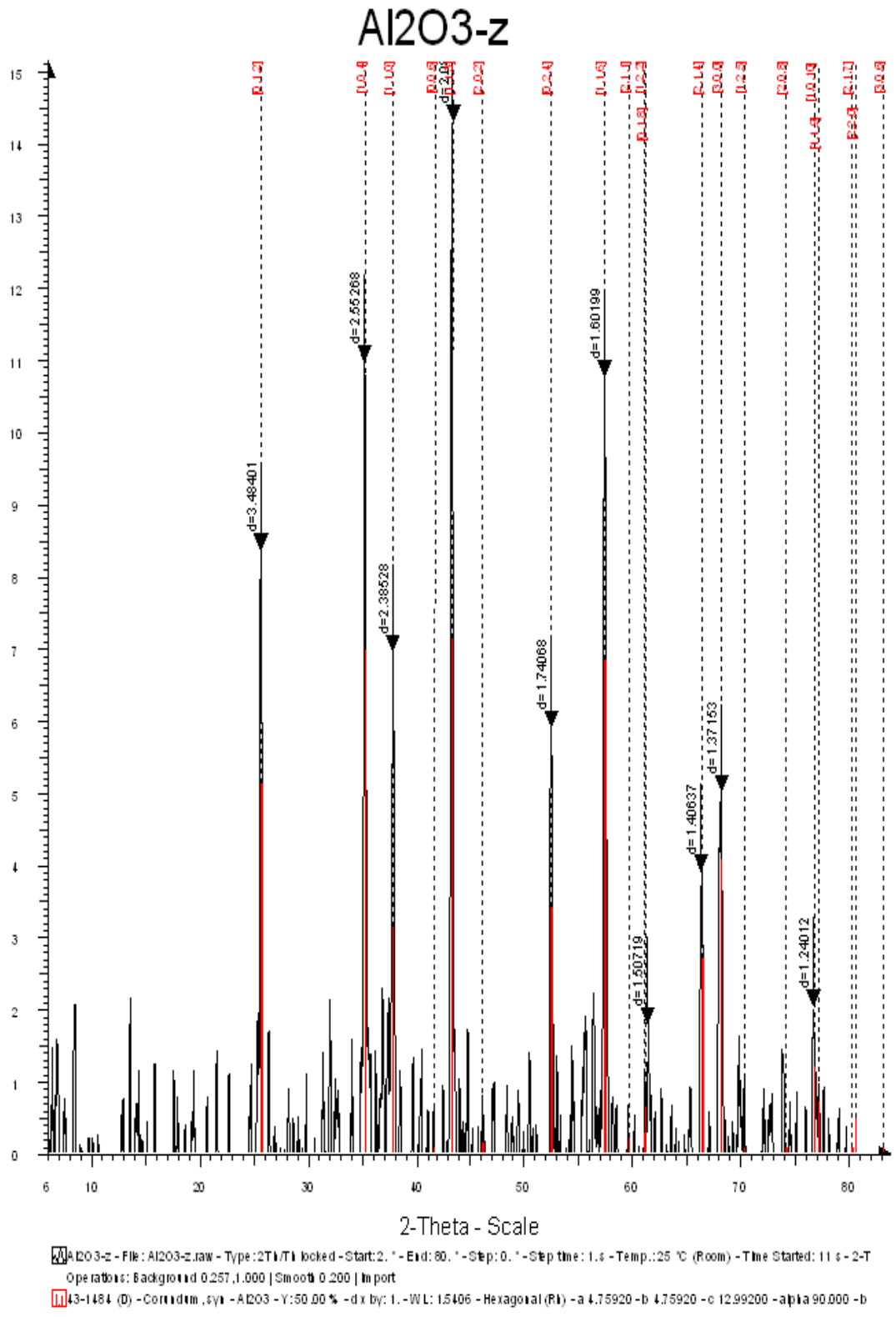

Figure 1 (c): XRD diffraction pattern of Al_2O_3 annealed at 1200°C

APPENDIX B

INTERFACIAL TENSION IFT MEASUREMENT

Abbreviations and units used in the list:

IFT_LY	: interface tension (Laplace - Young);
IFT_CSW	: interface tension (Cayias Schechter Wade);
F	: full shape;
L	: left side;
R	: right side;
C	: cylindrical part;
dDens	: density difference [g/cm³];
Vol	: volume [µl];
Err	: fitting error [pixel];
Speed	: rotation speed [1/min];
Alpha	: drop shape parameter alpha;
a	: drop curvature at apex [mm]

1. IFT of Oil – Al_2O_3 - S2

Run-No	IFT_LY	IFT_CSW	Err	Speed	Vol LY	Type
1	9.999	10.256	1.7	6999.5	5.977	F
2	10.143	10.403	1.8	6999.7	6.022	F
3	10.044	10.114	1.7	7000.7	6.022	F
4	9.848	9.974	3.4	7000.0	5.939	F
5	9.982	10.259	1.7	7000.2	5.976	F
6	9.837	9.830	2.0	7000.0	5.981	F
7	10.095	10.111	2.1	7000.1	6.067	F
8	10.129	10.260	1.8	6999.8	6.041	F
9	9.843	10.108	1.6	6999.3	5.933	F
10	10.124	10.251	1.8	6999.7	6.051	F
11	10.132	10.112	2.3	7000.1	6.089	F
12	9.913	9.971	3.6	6999.6	5.992	F
13	10.120	10.259	1.7	7000.3	6.033	F
14	9.841	9.973	3.4	6999.4	5.949	F
15	9.851	9.973	2.3	7000.4	5.954	F
16	9.857	10.112	1.9	7000.4	5.944	F
17	9.957	10.252	1.7	6999.8	5.980	F
18	9.862	9.968	1.9	7000.1	5.948	F
19	9.855	10.115	1.8	7000.2	5.957	F
20	9.975	9.967	2.0	6999.4	6.031	F
21	9.857	10.256	1.8	7000.3	5.942	F
22	9.987	9.969	2.3	6999.1	6.063	F
23	9.858	9.971	1.8	7000.4	5.970	F
24	9.996	10.244	1.9	6999.1	6.008	F
25	9.865	9.969	2.2	6999.5	5.965	F
26	9.977	9.973	2.1	7000.0	6.029	F
27	9.997	10.110	1.8	6999.6	6.009	F
28	9.858	10.111	1.9	6999.4	5.966	F
29	9.776	9.971	1.9	6999.7	5.936	F
30	9.983	10.108	2.1	6999.4	6.014	F
31	10.175	10.112	2.9	6999.5	6.129	F
32	9.702	9.973	2.5	6999.8	5.900	F
33	9.999	9.974	2.0	6999.6	6.005	F
34	9.848	9.967	1.8	7000.3	5.967	F
35	9.941	10.109	1.7	7000.1	6.001	F
36	9.968	10.259	1.8	6999.8	6.018	F
37	9.852	9.970	1.9	7000.4	5.968	F
38	9.986	10.256	2.6	7000.3	6.002	F
39	9.856	9.968	3.5	7000.3	5.971	F
40	9.861	9.829	2.0	7000.1	6.022	F
41	10.091	10.114	2.5	7000.4	6.026	F

Abbreviations and units used in the list: IFT_LY = interface tension (Laplace - Young); IFT_CSW = interface tension (Caylas Schechter Wade); F = full shape; L = left side; R = right side; C = cylindrical part; dDens = density difference [g/cm³]; Vol = volume [µl]; Err = fitting error [pixel]; Speed = rotation speed [1/min]; Alpha = drop shape parameter alpha; a = drop curvature at apex [mm]

2. IFT of Oil – Al_2O_3 - S3

Run-No	IFT_LY	IFT_CSW	Err	Speed	Vol LY	Type
1	9.999	10.256	1.7	6999.5	5.977	F
2	10.143	10.403	1.8	6999.7	6.022	F
3	10.044	10.114	1.7	7000.7	6.022	F
4	9.848	9.974	3.4	7000.0	5.939	F
5	9.982	10.259	1.7	7000.2	5.976	F
6	9.837	9.830	2.0	7000.0	5.981	F
7	10.095	10.111	2.1	7000.1	6.067	F
8	10.129	10.260	1.8	6999.8	6.041	F
9	9.843	10.108	1.6	6999.3	5.933	F
10	10.124	10.251	1.8	6999.7	6.051	F
11	10.132	10.112	2.3	7000.1	6.089	F
12	9.913	9.971	3.6	6999.6	5.992	F
13	10.120	10.259	1.7	7000.3	6.033	F
14	9.841	9.973	3.4	6999.4	5.949	F
15	9.851	9.973	2.3	7000.4	5.954	F
16	9.857	10.112	1.9	7000.4	5.944	F
17	9.957	10.252	1.7	6999.8	5.980	F
18	9.862	9.968	1.9	7000.1	5.948	F
19	9.855	10.115	1.8	7000.2	5.957	F
20	9.975	9.967	2.0	6999.4	6.031	F
21	9.857	10.256	1.8	7000.3	5.942	F
22	9.987	9.969	2.3	6999.1	6.063	F
23	9.858	9.971	1.8	7000.4	5.970	F
24	9.996	10.244	1.9	6999.1	6.008	F
25	9.865	9.969	2.2	6999.5	5.965	F
26	9.977	9.973	2.1	7000.0	6.029	F
27	9.997	10.110	1.8	6999.6	6.009	F
28	9.858	10.111	1.9	6999.4	5.966	F
29	9.776	9.971	1.9	6999.7	5.936	F
30	9.983	10.108	2.1	6999.4	6.014	F
31	10.175	10.112	2.9	6999.5	6.129	F
32	9.702	9.973	2.5	6999.8	5.900	F
33	9.999	9.974	2.0	6999.6	6.005	F
34	9.848	9.967	1.8	7000.3	5.967	F
35	9.941	10.109	1.7	7000.1	6.001	F
36	9.968	10.259	1.8	6999.8	6.018	F
37	9.852	9.970	1.9	7000.4	5.968	F
38	9.986	10.256	2.6	7000.3	6.002	F
39	9.856	9.968	3.5	7000.3	5.971	F
40	9.861	9.829	2.0	7000.1	6.022	F
41	10.091	10.114	2.5	7000.4	6.026	F

Abbreviations and units used in the list: IFT_LY = interface tension (Laplace - Young); IFT_CSW = interface tension (Caylas Schechter Wade); F = full shape; L = left side; R = right side; C = cylindrical part; dDens = density difference [g/cm³]; Vol = volume [µl]; Err = fitting error [pixel]; Speed = rotation speed [1/min]; Alpha = drop shape parameter alpha; a = drop curvature at apex [mm]

3. IFT of Oil – Al_2O_3 - SA-S4

Run-No	IFT_LY	IFT_CSW	Err	Speed	Vol LY	Type
1	11.432	11.331	2.0	4800.1	24.875	F
2	11.462	11.332	1.7	4800.1	24.897	F
3	11.452	11.330	1.7	4800.1	24.878	F
4	11.494	11.456	1.5	4800.1	24.898	F
5	11.480	11.455	1.3	4800.1	24.827	F
6	11.468	11.325	1.8	4799.2	24.965	F
7	11.514	11.329	2.1	4800.1	25.055	F
8	11.522	11.454	1.6	4800.1	24.961	F
9	11.512	11.461	1.3	4801.1	24.883	F
10	11.482	11.331	1.8	4800.1	24.985	F
11	11.540	11.456	1.6	4800.1	24.997	F
12	11.521	11.333	2.3	4800.2	25.067	F
13	11.538	11.455	1.7	4800.1	24.994	F
14	11.517	11.453	1.7	4800.1	24.951	F
15	11.527	11.455	1.5	4800.1	24.970	F
16	11.361	11.455	3.0	4800.1	24.627	F
17	11.482	11.454	1.5	4800.1	24.916	F
18	11.522	11.454	1.5	4800.1	24.960	F
19	11.534	11.329	2.2	4800.1	25.098	F
20	11.503	11.453	1.7	4800.1	24.963	F
21	11.496	11.457	1.5	4801.1	24.939	F
22	11.460	11.453	1.3	4800.1	24.870	F
23	11.496	11.454	1.5	4800.1	24.946	F
24	11.480	11.452	1.4	4800.1	24.914	F
25	11.474	11.455	1.4	4800.1	24.899	F
26	11.506	11.452	1.5	4800.0	24.971	F
27	11.518	11.450	1.5	4799.2	24.961	F
28	11.474	11.449	1.6	4799.2	24.908	F
29	11.511	11.448	1.5	4799.2	24.990	F
30	11.492	11.454	1.6	4800.1	24.937	F
31	11.514	11.453	1.5	4800.1	24.944	F
32	11.485	11.453	1.4	4800.1	24.923	F
33	11.493	11.455	1.6	4800.1	24.940	F
34	11.509	11.456	1.5	4800.1	24.974	F
35	11.525	11.454	1.5	4800.1	25.010	F
36	11.480	11.453	1.4	4800.1	24.913	F
37	11.437	11.454	1.3	4800.1	24.817	F
38	11.477	11.454	1.4	4800.1	24.906	F
39	11.478	11.453	1.6	4800.1	24.949	F
40	11.470	11.453	1.5	4800.1	24.934	F
41	11.458	11.453	1.5	4800.1	24.825	F
42	11.472	11.454	1.5	4800.1	24.894	F
43	11.424	11.454	1.5	4800.1	24.832	F

Abbreviations and units used in the list: IFT_LY = Interface tension (Laplace - Young); IFT_CSW = Interface tension (Caylas Schechter Wade); F = full shape; L = left side; R = right side; C = cylindrical part; dDens = density difference [g/cm³]; Vol = volume [µl]; Err = fitting error [pixel]; Speed = rotation speed [1/min]; Alpha = drop shape parameter alpha; a = drop curvature at apex [mm]